1

Direct and resonant double photoionization: from atoms to solids

LORENZO AVALDI AND GIOVANNI STEFANI

1.1 Introduction

Electron–electron correlation plays a crucial role in determining physical and chemical properties in a wide class of materials that exhibit fascinating properties including, for example, high-temperature superconductivity, colossal magnetoresistance, metal insulator or ferromagnetic anti-ferromagnetic phase transitions, self assembly and quantum size effects. Furthermore, electron–electron correlation governs the dynamics of charged bodies via long-range Coulomb interaction, whose proper description constitutes one of the more severe tests of quantum mechanics.

Nevertheless, the effects due to correlation remain rather elusive for almost all of the experimental methods currently used to investigate matter in its various states of aggregation. Indeed, being related to processes with two active electrons, like satellite structures in photoemission (i.e., ionization processes with one ejected and one excited electron), or double ionization events, they influence marginally the spectral responses of the target, that are primarily determined by single and independent particle behaviours. Hence the experimental effort devoted in the last 30 years to develop a new class of experiments, whose spectral response is determined mainly by the correlated behaviour of electron pairs.

The common denominator of this class of experiments is the study of reactions whose final state has two holes in the valence orbitals and two unbound electrons in the continuum. It is exactly through interaction of these holes and electron pairs that correlation shapes the cross section of the double ionization processes.

The archetypal processes that create hole pairs are the direct valence double photoionization (DPI) and the core-hole Auger decay. In both cases, the Coulomb interaction between valence electrons is responsible for the promotion either of
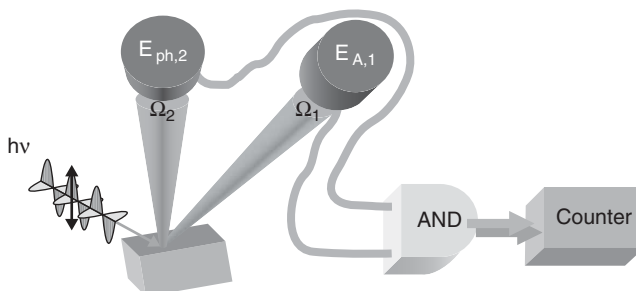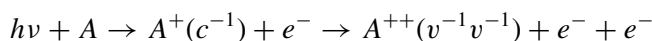

Figure 1.1 Scheme of an electron–electron coincidence experiment.

valence electron pairs to the continuum, in the DPI case, or for the core-hole decay
with emission of an Auger electron that is paired to the photoelectron from core
ionization. In both cases, experiments designed to study these events detect the
unbound electron pairs after energy and momentum selection.

The prototypal scheme for such experiments is **1-photon IN** and **2-electrons
OUT**, i.e.,

$$h\nu + A \rightarrow A^{++}(v^{-1}v^{-1}) + e^- + e^-$$
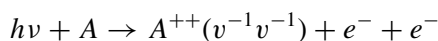
in the case of DPI, and

$$h\nu + A \rightarrow A^+(c^{-1}) + e^- \rightarrow A^{++}(v^{-1}v^{-1}) + e^- + e^-$$

in the case of Auger decay.

It is evident that both processes share a similar, sometimes identical, final doubly
charged ion state. These two schemes also clarify the characteristic observables
of this class of experiments, i.e., the energy and momentum (emission angle)
distributions of the final electron pair.

These distributions are determined by measuring the kinetic energy and momen-
tum of the individual electrons and by correlating them in time in order to discrim-
inate the pairs generated in the same event from the ones generated in independent
events. This is done by detecting the final electron pairs with an apparatus whose
scheme of principle is given in Fig. 1.1.

Since their first introduction by Haak *et al*. [1], 1-photon IN and 2-electrons
OUT experiments have been applied extensively to atoms, molecules and, more
recently, solids. The experimental challenge is due to the small cross section of
these processes. This handicap has been overcome on the one hand by the advent
of the high intensity third-generation synchrotron radiation sources [2], and on the
other hand by the development of highly sophisticated set-ups [3] which allow
the simultaneous detection of electrons with several energies over a large solid
angle. Together with the complementary approach where one or two electrons are

detected in coincidence with the recoil ion [4], these experiments have yielded detailed information on electron correlations in both bound and unbound states. A few relevant study cases on either aggregation state are presented and discussed in the following.

1.2 Direct double photoionization

Two electron systems, like the He atom and H_2 molecule, represent the most suited targets to investigate the dynamics of the direct emission into the continuum of two electrons following the absorption of a VUV or soft X-ray photon. Therefore Sections 1.2.1 and 1.2.2 will be devoted to the presentation of selected experimental results in He and H_2 and to the present understanding of direct DPI. For atoms heavier than He, the complexity of their initial states is reflected in a large variety of patterns for the coincidence angular distributions produced in a DPI event. However, the basic understanding of the DPI process in these systems can be traced back to the one in He, thus we have decided to limit this chapter to two electron systems. A review of the DPI results in the heavier rare gases can be found in [5].

Section 1.2.3 is devoted to the description of the results of direct DPI on solids and shows how DPI discloses the possibility to investigate directly the electron correlation in the bands, as well as providing evidence of the exchange-correlation hole.

1.2.1 The He atom

The archetypal system to study direct DPI is the He atom. In this two-electron system the absorption of a photon with energy larger than 79.004 eV [6], the He double-ionization potential I^{2+}, may lead to a bare nucleus and two free electrons:

$$h\nu + \text{He} \rightarrow \text{He}^{2+} + e^- + e^-. \tag{1.1}$$
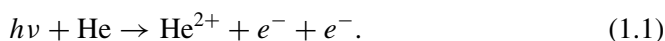
In the simplest case where the incoming photon is linearly polarized along a well-defined direction, $\boldsymbol{\varepsilon}$, then the latter represents the natural quantization axis. The final state is fully characterized by the momenta $\mathbf{k}_1$ and $\mathbf{k}_2$ or, alternatively, by their kinetic energies E_1 and E_2 and the spherical angles $\Omega_1(\theta_1, \phi_1)$, $\Omega_2(\theta_2, \phi_2)$ of the two electrons, where $\theta_i(i = 1, 2)$ is the angle with respect to $\boldsymbol{\varepsilon}$ and ϕ_i the angle with respect to the plane which contains the axes of polarization and of the photon beam. The excess energy $E = h\nu - I^{2+}$ is shared between the two electrons according to $E = E_1 + E_2$. From dipole selection rules in (1.1) the symmetry of the electron pair is well defined, $^1P^0$, and the quantum numbers of the electron pair are $L = 1$, $M = 0$, $S = 0$ and parity $\pi = $ odd.

The quantities which describe the process (1.1) are: its total cross section σ, the singly differential cross section $\frac{d\sigma}{dE_1}(0 \le E_1 \le E)$, which gives the energy distribution of the ejected photoelectrons, the doubly differential cross section $\frac{d^2\sigma}{dE_1 d\Omega_1}$, which describes the angular distribution of each one of the two photoelectrons, and finally the triply differential cross section $\frac{d^3\sigma}{dE_1 d\Omega_1 d\Omega_2}$, which describes the correlated motion of the electron pair for a fixed energy sharing $R = \frac{E_2}{E_1}$. The questions to be answered concern the shape and absolute value of the total DPI cross section, the way the two ejected electrons share the excess energy E and the shape of the correlated angular distribution of the two electrons.

The shape of the total cross section for DPI of He and its ratio to the one of single photoionization have been well characterized both experimentally and theoretically [7]. The cross section increases from threshold ($\sigma = 1.021 \pm 0.005$ kb at $E = 1$ eV [8]) up to a broad maximum at about $E = 20$ eV, where it has a value of about 10 kb [9] and then it decreases continuously. The increase from threshold to about 2 eV above it follows a power law E^n, with an exponent $n = 1.05 \pm 0.02$ [8], in good agreement with $n = 1.056$, as predicted by Wannier [10] from a classical analysis of the dynamics of double escape. The small value of the cross section and the behaviour near threshold are a clear indication of the role of electron correlation in the process, and indicate that close to threshold the double escape of two electrons is very unlikely, as each of them tends to be attracted back to the nucleus.

While a plethora of measurements of the $\frac{d^3\sigma}{dE_1 d\Omega_1 d\Omega_2}$ at different E and R values have been reported [5], less attention has been paid to the measurements of $\frac{d\sigma}{dE_1}$ and $\frac{d^2\sigma}{dE_1 d\Omega_1}$, which have been measured mainly via time-of-flight techniques [11–13]. The energy distribution $\frac{d\sigma}{dE_1}$ is flat in the threshold region and assumes a U shape at higher E. The flatness in the threshold region is a direct consequence of the ergodic character of the dynamics in this energy region, while the U shape near the maximum of the σ and at higher E means that the unequal energy sharing becomes more likely than the equal sharing. The doubly differential cross section,

$$\frac{d^2\sigma}{dE_1 d\Omega_1} = \frac{d\sigma}{dE_1}\frac{[1 + \beta(E_1) P_2(\cos\theta_1)]}{4\pi}, \qquad (1.2)$$

is the product of the singly differential cross section by an angular factor depending upon the asymmetry parameter β and the second-order Legendre polynomial P_2. The measurement of the evolution of β with E, which depends on the radial matrix element for the dipole-allowed transitions, is a sensitive probe of the photoionization dynamics. Wehlitz *et al.* [11] in a series of measurements at $10 \le E \le 41$ eV showed that β varies with the ratio $\frac{E_2}{E_1}$. This is consistent with the analysis

performed by Maulbetsch and Briggs [14], who also proved that only in the case
where this ratio is kept fixed as $E \to 0$ then β approaches the limiting value of -1,
expected from a classical analysis of the dynamics of double escape [15, 16].

Finally, for a radiation linearly polarized along the $\boldsymbol{\varepsilon} = \varepsilon\mathbf{x}$ axis, taking into
account the invariance with respect to the rotation about a preferential symmetry
axis [15], the triply differential cross section for emission of the two electrons is
given exactly by:

$$\frac{d^3\sigma}{dE_1 d\Omega_1 d\Omega_2} = |a_{\mathrm{g}}(E_1, E_2, \theta_{12})(\cos\theta_1 + \cos\theta_2)$$
$$+ a_{\mathrm{u}}(E_1, E_2, \theta_{12})(\cos\theta_1 - \cos\theta_2)|^2, \qquad (1.3)$$

where $a_{\mathrm{g}}(E_1, E_2, \theta_{12})$ and $a_{\mathrm{u}}(E_1, E_2, \theta_{12})$ are two complex amplitudes (respec-
tively symmetric and antisymmetric in the exchange $E_1 \leftrightarrow E_2$), which resume the
dynamics of the pair. Accordingly, these amplitudes only depend on the energies
and mutual angle θ_{12} of the two electrons. The other factors $(\cos\theta_1 \pm \cos\theta_2)$ result
from the description of the photon–atom interaction within the dipole approxima-
tion. They are known as angular factors as they derive from the $L = 1$, $M = 0$
character of the final state. Whenever another type of polarization is used in the
experiment, Eq. (1.3) is to be changed in its angular factors, but the amplitudes
remain the same. The above expression allows the classification of the experiments
into equal ($E_1 = E_2$) and unequal ($E_1 \neq E_2$) sharing subsets. For equal sharing,
$\frac{d^3\sigma}{dE_1 d\Omega_1 d\Omega_2}$ reduces to:

$$\frac{d^3\sigma}{dE_1 d\Omega_1 d\Omega_2} = \left|a_{\mathrm{g}}(E/2, E/2, \theta_{12})\right|^2 (\cos\theta_1 + \cos\theta_2)^2. \qquad (1.4)$$

Equation (1.4) clearly shows that back-to-back emission in equal sharing is forbid-
den, as can be immediately verified, because $\mathbf{k}_2 = -\mathbf{k}_1$ implies $\theta_2 = \pi - \theta_1$, and
therefore $\frac{d^3\sigma}{dE_1 d\Omega_1 d\Omega_2} = 0$. Another point can now be outlined: the amplitudes $a_{\mathrm{g,u}}$
themselves should rather be maxima for back-to-back emission ($\theta_{12} = \pi$), because
the electron–electron repulsion should drive the electrons to opposite directions
with respect to the ion. From these simple ideas it was predicted [15], before any
experiment on He became feasible, that from the competition of the two factors
the differential cross section in Eq. (1.4) should have a 'butterfly' shape in polar
coordinates (Fig. 1.2). If the first factor in Eq. (1.4) is replaced by a Gaussian func-
tion, which has the property to be maximum at $\theta_{12} = \pi$ as expected for physical
reasons,

$$\left|a_{\mathrm{g}}(E/2, E/2, \theta_{12})\right|^2 = a(E)\exp[-4\ln2(\theta_{12} - \pi)^2/\theta_{1/2}{}^2], \qquad (1.5)$$

where $a(E)$ is a scaling factor and $\theta_{1/2}$ the width of the Gaussian at half maximum,
then all experiments can be fitted as a function of a single parameter: $\theta_{1/2}$. The

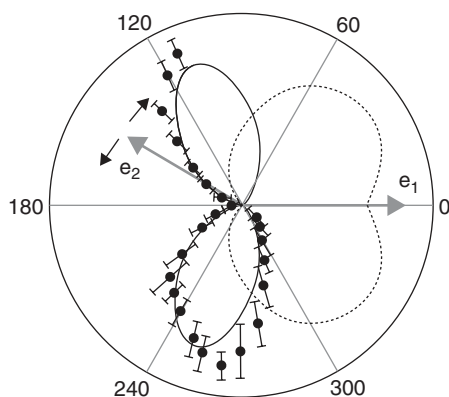6   *Lorenzo Avaldi and Giovanni Stefani*

Figure 1.2 Triply differential cross sections at $E = 20$ eV, and equal sharing $E_1 = E_2 = 10$ eV, from Turri *et al.* [17]. The full curve is a fit using Eqs. (1.4) and (1.5) and $\theta_{1/2} = 90 \pm 3°$. The dotted curve uses the same expressions but the value of $\theta_{1/2}$ deduced from the Wannier law.

Gaussian function in Eq. (1.5) is supported by the theory of Wannier, but only in the threshold region [18]. However, Kheifets and Bray [19] numerically proved that the Gaussian ansatz appears to be a suitable representation of the a_{g} amplitude up to $E = 80$ eV and experimentally a significant breakdown of this representation has not been reported so far. The width parameter $\theta_{1/2}$ gives the strength of angular correlations between the two electrons at equal sharing: these correlations are the highest when $\theta_{1/2}$ is small, the lowest when $\theta_{1/2}$ is large. The fits to the measured $\frac{d^3\sigma}{dE_1 d\Omega_1 d\Omega_2}$ (Fig. 1.3) leads to values of $\theta_{1/2}$, which increase smoothly from $57 \pm 4°$ at $E = 0.1$ eV to $120 \pm 4°$ at $E = 80$ eV. At the highest energy $E = 450$ eV, the equal sharing DPI is observed to be very weak [23], and has not been measured. The predicted value of the width from Wannier theory is $\theta_{1/2} = 91\, E^{0.25}$ (units in degrees for $\theta_{1/2}$ and eV for E), which, as expected, is consistent with experiments only at the lowest energies $E = 0.1$ and 0.2 eV, but overestimates the experimental values already at $E = 1$ eV and gives much too large values at higher energy, as illustrated in Fig. 1.3. The results of the equal energy sharing experiments can be summarized by saying that the angular correlations repelling the two electrons into opposite directions are very intense at threshold, as expected from the theory of Wannier, and then progressively relax as E increases, until equal sharing DPI becomes practically negligible at very high E. These high-energy experiments, where the three-body effects in the final state become negligible, are the ones proposed in the seventies by Neudatchin *et al.* [24] to investigate directly electron correlations in the initial state and therefore to discriminate among different bound state wave functions, which adopt different representation of electron correlations. Unfortunately, this unique property of the $\frac{d^3\sigma}{dE_1 d\Omega_1 d\Omega_2}$ could not be
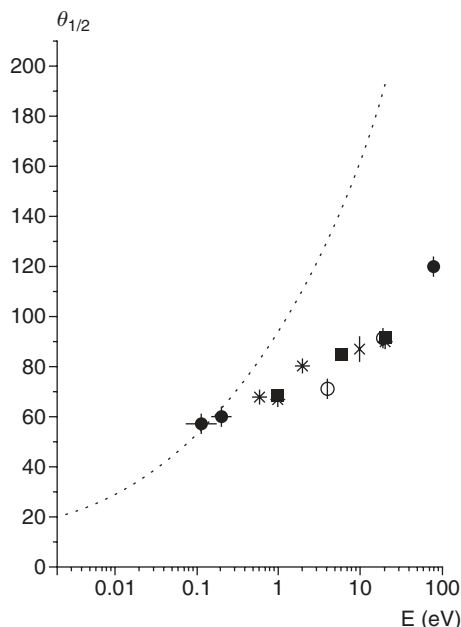
Figure 1.3 Experimental values of the width $\theta_{1/2}$ from fits of Eqs. (1.4) and (1.5) to the measured equal sharing triply differential cross sections. The dotted curve shows the $\theta_{1/2} = 91\ E^{0.25}$ Wannier law. Experimental data by Huetz and Mazeau [20] (dots with uncertainty on the energy scale), Dawber *et al.* [21] (stars), Huetz *et al.* [22] (open circles), Schwarzkopf *et al.* [2] (full squares) and Turri *et al.* [17] (dots).

explored experimentally due to the vanishing values of the cross section, too small even for the present multi-angle and multi-energy set-ups [23].

For unequal sharing, both amplitudes are expected to contribute, leading to more complicated shapes, as shown in Figs. 1.4 and 1.5. However, Eq. (1.3) still provides a guide to disentangle the various effects, and methods have been developed to extract the amplitudes from experiments. This is especially instructive as the amplitudes are the natural quantities to be calculated from *ab initio* theories. Before addressing this topic, here is a qualitative description of the evolution of the shape of the $\frac{d^3\sigma}{dE_1 d\Omega_1 d\Omega_2}$ as E increases. In the region near threshold, Lablanquie *et al.* [3] and Dawber *et al.* [21] reported no significant changes or new features for R up to 12.3. The measured $\frac{d^3\sigma}{dE_1 d\Omega_1 d\Omega_2}$ look almost the same at all the different energy sharings: a node continues to exist at $\theta_{12} = 180°$ even for $E_1 \neq E_2$ and indeed the data look very similar to the equal energy case. These observations demonstrate that a_u remains small compared to a_g and a_g is almost independent of R. Qualitatively, these findings depend on the fact that, close to threshold, double escape of the two electrons is very unlikely, as each of them tends to be attracted
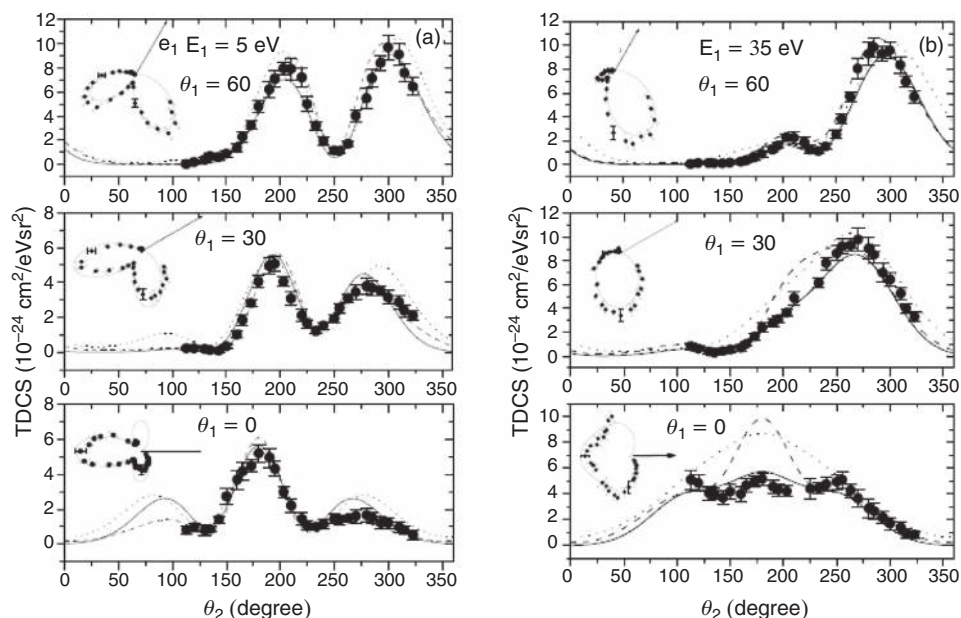
　　　　　　　　　　Lorenzo Avaldi and Giovanni Stefani

Figure 1.4 Triply differential cross sections from Bolognesi *et al.* [25] at $E = 40$ eV, and $\theta_1 = 0°, 30°, 60°$. (a) $E_1 = 5$ eV ($R = 7$); (b) complementary kinematics: $E_1 = 35$ eV ($R = 0.14$). The CCC and 3C calculations are plotted as dashed and dotted lines, respectively. The full line is a representation of the TDCS according the parameterization by Cvejanovic and Reddish [26]. Both cartesian coordinates and polar coordinates (small insets) are used.

back to the nucleus and the system has to maintain itself along the Wannier ridge ($r_1 \approx r_2$). At larger E, both amplitudes are now significant and they lead to the complicated shapes displayed in Figs. 1.4 and 1.5. A large number of experiments have been performed in this energy domain. The two examples selected and shown in Figs. 1.4 and 1.5 illustrate quite well the advantages and disadvantages of the different experimental methods. The momentum imaging COLTRIMS method [28] gives the absolute $\frac{d^3\sigma}{dE_1 d\Omega_1 d\Omega_2}$ for all angles (only $\theta_1 = 30°$ is shown in Fig. 1.5) and all R values at once [27]. The multi-analyzer technique [25, 29] (Fig. 1.4) usually produces less data on a relative scale only, but each of them can be monitored individually to reach the desired statistics, and indeed the figure shows that excellent statistics have been achieved.

The main effect of the antisymmetric amplitude a_u is that the back-to-back emission is no longer forbidden, as shown in Fig. 1.4. Moreover, considering the two complementary kinematics obtained by exchanging $E_1 \leftrightarrow E_2$ and the properties of the amplitudes, one observes that the difference between the two
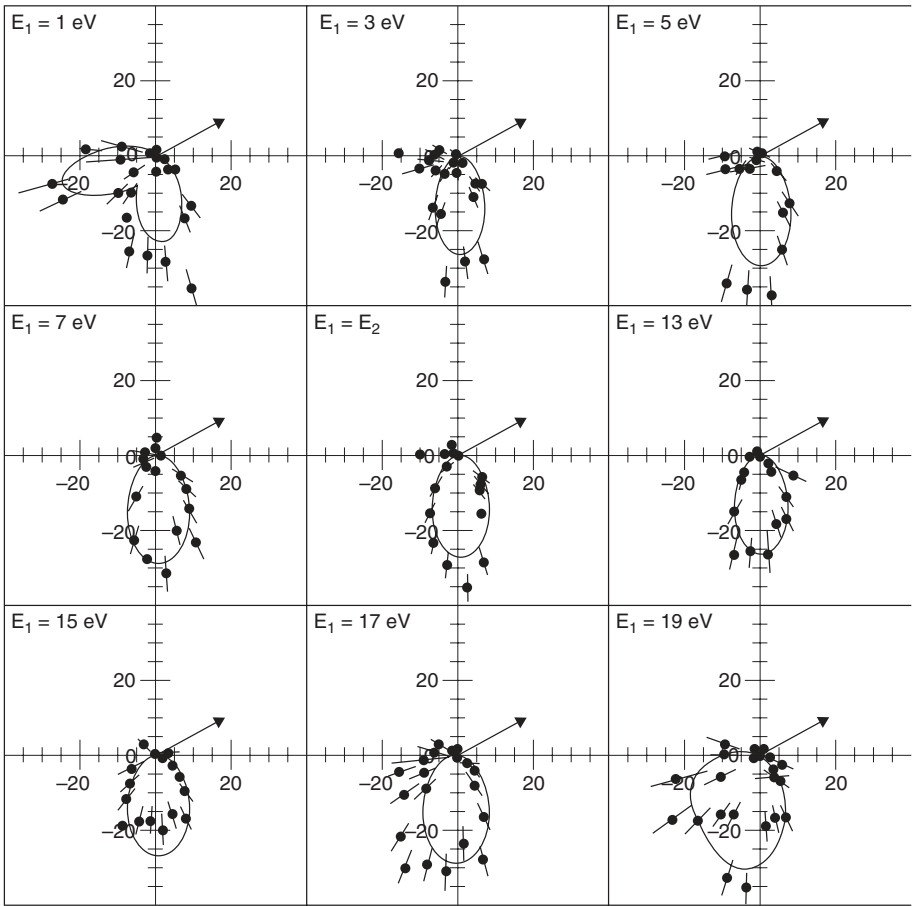
Figure 1.5 Absolute triply differential cross sections (barn $eV^{-1}sr^{-2}$) measured by Bräuning *et al.* [27] at $E = 20$ eV, and $\theta_1 = 30°$ with the COLTRIMS momentum imaging technique. Nine values of E_1 are reported, and CCC calculations are compared with the experiments on absolute scale (full line).

triply differential cross sections,

$$\Delta = \frac{d^3\sigma(E_2, E_1)}{dE_1 d\Omega_1 d\Omega_2} - \frac{d^3\sigma(E_1, E_2)}{dE_1 d\Omega_1 d\Omega_2} = \left|a_g\right| |a_u| \cos\delta \left(\cos\theta_2^2 - \cos\theta_1^2\right), \quad (1.6)$$

is completely determined by the phase difference δ between the two amplitudes. This is responsible for the different shapes that are observed when fixing in space either the highest, or the lowest energy electron (Fig. 1.4). At higher energy ($h\nu = 530$ eV) Knapp *et al.* [23, 30, 31] showed that the dynamics of the electron pair becomes much simpler. This is not surprising as, in general, high kinetic energies

of the particles mean that their interaction becomes less important, and therefore three-body effects in the final state tend to be washed out. Two-step mechanisms have been envisaged for the double photoionization process in this region. The first one is the shake-off, where almost all energy is transferred to a quickly removed electron. This leaves a state which is not an eigenstate of the ion, and therefore has a component within the double continuum. Consequently, the second electron can be removed, but with low correlation to the first one. The experimental results show that this shake-off process dominates over the other proposed mechanism, named TS1 [32], in which the first high-energy electron kicks out a second one, leading to an angular correlation around $\theta_{12} = 90°$, as in hard spheres elastic collisions.

Berakdar and Klar [33] and Berakdar *et al.* [34] predicted that He $\frac{d^3\sigma}{dE_1 d\Omega_1 d\Omega_2}$ measured with circularly polarized radiation should display a helicity dependence, i.e., a non-vanishing circular dichroism, CD. This is because, due to parity conservation, the helicity of the incident photon is transferred to the three-body system, the He atom, and the continuum spectrum of this excited system depends on the helicity of the absorbed photon. Using the same representation as for Eq. (1.3), but taking the quantization axis along the photon beam, the $\frac{d^3\sigma}{dE_1 d\Omega_1 d\Omega_2}$ for right, R, and left, L, circular polarizations is given by:

$$\frac{d^3\sigma_{\rm L}}{dE_1 d\Omega_1 d\Omega_2} = |(a_{\rm g}(E_1, E_2, \theta_{12}) + a_{\rm u}(E_1, E_2, \theta_{12})) \sin \theta_1 e^{-i\varphi_1}.$$

$$+ (a_{\rm g}(E_1, E_2, \theta_{12}) - a_{\rm u}(E_1, E_2, \theta_{12})) \sin \theta_2 e^{-i\varphi_2}|^2. \quad (1.7)$$

$$\frac{d^3\sigma_{\rm R}}{dE_1 d\Omega_1 d\Omega_2} = |(a_{\rm g}(E_1, E_2, \theta_{12}) + a_{\rm u}(E_1, E_2, \theta_{12})) \sin \theta_1 e^{+i\varphi_1}$$

$$+ (a_{\rm g}(E_1, E_2, \theta_{12}) - a_{\rm u}(E_1, E_2, \theta_{12})) \sin \theta_2 e^{+i\varphi_2}|^2. \quad (1.8)$$

The circular dichroism (CD) is given by the difference:

$$\mathrm{CD} = \frac{d^3\sigma_{\rm L}(E_2, E_1)}{dE_1 d\Omega_1 d\Omega_2} - \frac{d^3\sigma_{\rm R}(E_1, E_2)}{dE_1 d\Omega_1 d\Omega_2}$$

$$= -4 \left|a_{\rm g}(E_1, E_2, \theta_{12})\right| |a_{\rm u}(E_1, E_2, \theta_{12})| \sin \delta \sin \theta_1 \sin \theta_2 \sin (\varphi_2 - \varphi_1), \quad (1.9)$$

where δ is the phase difference between the two amplitudes, as in Eq. (1.6). At equal energy sharing, $|a_{\rm u}| = 0$ and the CD cancels. This is not surprising as the momenta of the two electrons are then indistinguishable and cannot constitute, with the photon beam, an oriented system. Equation (1.9) shows that the CD is directly related to the phase difference between the two amplitudes. The same holds for the difference Δ of the triply differential cross sections under linear polarization (Eq. (1.6)). It is worth noting that these quantities are both necessary for a complete determination of δ. They also constitute a severe test of *ab initio* theories, as they